Characteristics of 3D Printed Plastic Scintillator for Thermal Neutron Measurement with Pulse Shape Discrimination

Kyungmin Kim · Dong Geon Kim · Sangmin Lee · Jaebum Son · Yong Kyun Kim*
Department of Nuclear Engineering, Hanyang University, Seoul 04763, Korea
*E-mail: ykkim4@hanyang.ac.kr

Introduction

Neutron detectors based on ^{3}He have large increased in use demand for homeland security and basic research [1]. Therefore, alternative technologies to replace ^{3}He such as have actively been studied. Plastic scintillator, which is capable of neutron detection, is considered one of the alternatives. Since neutron fields are typically present with γ-ray and plastic scintillators have relatively high γ-ray sensitivity, those require neutron-gamma (n-γ) separation technique such as pulse shape discrimination (PSD) methods. PSD capability of general plastic scintillators based on polyvinyltoluene (PVT) is known to be possible at 20-30wt% of 2,5-diphenyloxazole (PPO) although to be difficult at 1-5wt% [2]. Plastic scintillator is one of the organic scintillator types, and they can be manufactured by 3D printing techniques. The advantages of the technique are simple way, fast production, low cost and customizing easily. In previous study, PSD capability of 3D printed scintillators based on acrylic monomer according to PPO concentration had been confirmed, and it was also possible with 2wt% PPO [3]. In this study, PSD was attempted using 3D printed plastic scintillators for separating thermal neutron. Thermal neutrons are typically measured using secondary particles through nuclear reaction, and ^{6}LiF had been doped for the reaction. The ^{6}Li has advantages such as reasonable neutron capture cross-section, relatively high energy released in the capture reaction, as well as the absence of γ-ray through secondary particles [4]. The fabricated scintillators were evaluated through relative light output (LO) and figure of merit (FOM). In the research of Zaitseva et al. [5], the FOM was analyzed as a useful PSD performance when is greater than 1.27.

Materials and Methods

1. Fabrication of 3D Printed Plastic Scintillator

3D printer (Asiga-PICO 2HD UV385) based on digital light processing (DLP) technique was used for fabrication of scintillators, and it is relatively fast with top-down stacking structure. Each 3D printed scintillator was fabricated to cylindrical and diameter of 25 mm and height of 10 mm. The resins for 3D printed scintillators were composed of 1.5wt%-PPO. ^{6}Li concentration were 0wt% and 0.05wt%. Fig. 1 presents the configuration of 3D printer.

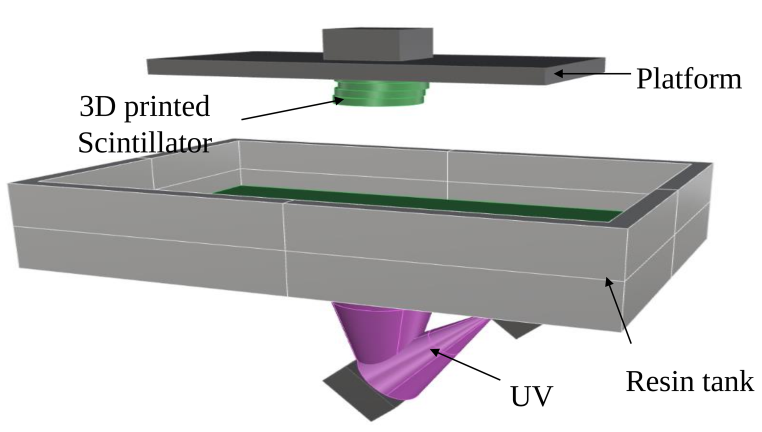

Fig. 1. Configuration of 3D printed based on DLP technique.

2. Energy Calibration

The plastic scintillators were connected to PMT (Hamamatsu-H6410) with -1400 V of high-voltage. The charge signals were delivered to Flash-ADC (Notice-NGT400). Data acquisition were sent to an online PC with the ROOT software framework through Ethernet. In this study, the scintillators were calibrated using three Compton edges of ^{137}Cs (477.65 keV) and ^{22}Na (340.67 keV and 1061.67 keV). The measurement system and results are shown in Fig. 2 below.

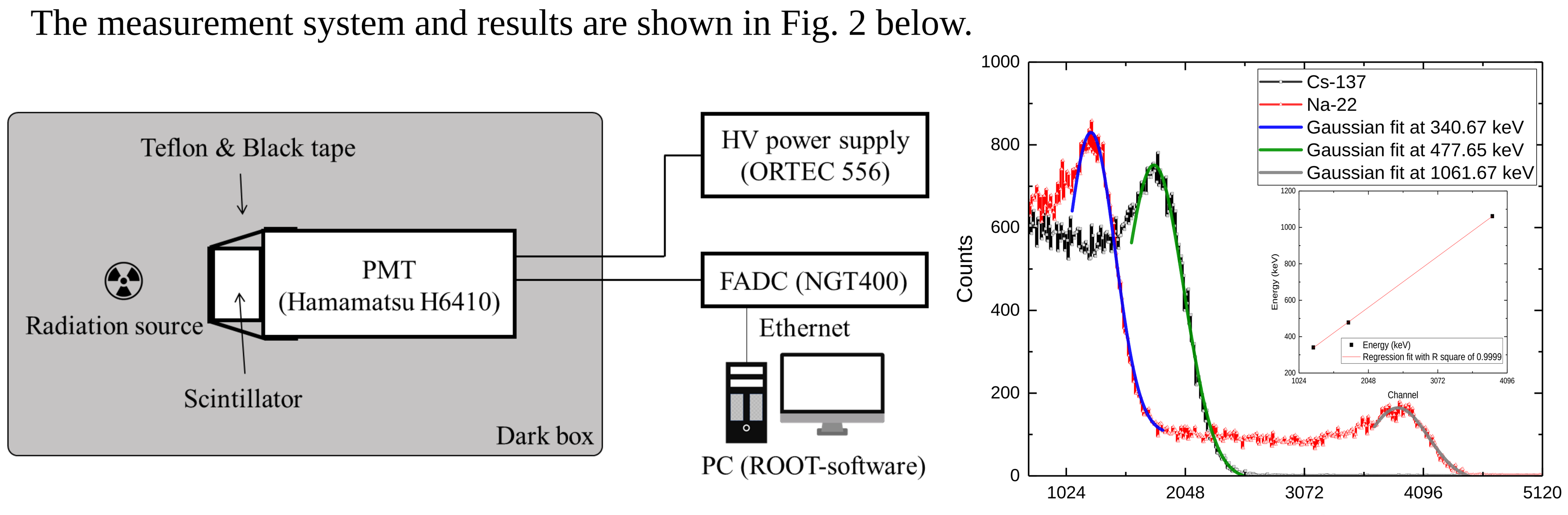

Fig. 2. Schematic diagram of the measurement system (left) and Energy spectra of 3D printed scintillator doped with 0.05wt%-^{6}Li for ^{137}Cs and ^{22}Na (right).

3. Relative Light Output

LO is calculated using the correlation between light yield, which consist of energy peak positions and gain of amplifier, and effective quantum efficiency (Q.E.$_{eff}$). The equation is given by the following equation (1):

$$Light\ output = \frac{PP_E}{K_E} \times \frac{PP_{1phe}}{K_{1phe}} \times \frac{1}{E_{compton\ edge}} \times \frac{1}{Q.E._{eff}}\ [ph/MeV] \qquad (1)$$

PP_E: specific of energy peak position　K_E: gain of amplifier　$E_{compton\ edge}$: Compton edge energy
PP_{1phe}: single photoelectron peak position　K_{1phe}: gain of amplifier　$Q.E._{eff}$: effective quantum efficiency

LY was defined by the number of photoelectrons per energy unit. This is generally derived from using single photoelectron peak position and specific of energy peak position with each gain of amplifier. It was calculated using the ^{137}Cs energy spectrum measured through the equal voltage and gain, easily.

The effective quantum efficiency was derived through calculation between quantum efficiency of PMT and emission intensity of scintillators. Emission wavelength of each scintillators were measured using the fluorescence spectrophotometer (Cary Eclipse, Varian), respectively. The spectra of emission wavelength and quantum efficiency of H6410 are shown in Fig. 3.

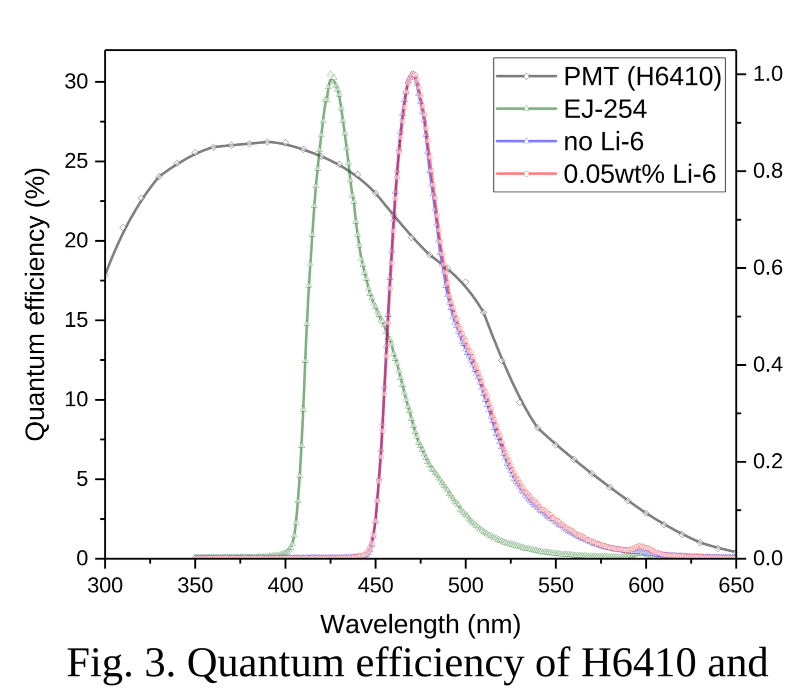

Fig. 3. Quantum efficiency of H6410 and emission intensity according to wavelength.

4. Figure of Merit

FOM was evaluated in energy region of thermal neutron spectrum . The values used for calculation of FOM are shown in the Fig. 4. FOM was defined by following equation (2):

$$FOM = \frac{S}{FWHM_{gamma} + FWHM_{neutron}} \qquad (2)$$

S: Distance between mean ΔQ/Q neutron and γ-ray
FWHM: Full width half at maximum

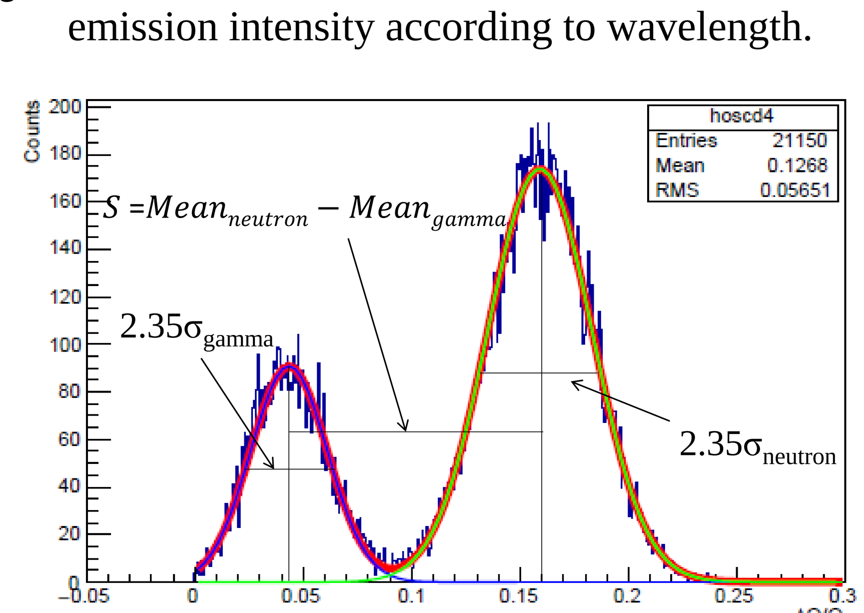

Fig. 4. Detailed meaning of the FOM value (x-axis: PSD factor means ratio of body and tail in spectrums, y-axis: counts).

Results and Discussion

Q.E.$_{eff}$ and Light output

The relative LO of 3D printed scintillator without ^{6}Li against EJ-254 was 139.2%. The LO of scintillator doped with 0.05wt%-^{6}Li decreased by 1%. The calculated Q.E.$_{eff}$ and LO are shown in Table I.

Table I. Effective quantum efficiency and light output

Scintillator	Q.E.$_{eff}$ [%]	Light output [ph/MeV]
EJ-254	23.29	7178.03
no ^{6}Li	17.75	9991.53
0.05wt% ^{6}Li	18.01	9894.81

Figure of Merit

^{252}Cf (77 μCi) source was used for neutron irradiations of this work. In order to reduce γ-ray and moderate fast neutron, the 5 cm lead and polyethylene were located in front of ^{252}Cf.

In order to separate n-γ, the charge comparison, which is one of PSD methods, was used. The ΔQ/Q of total and partial of pulse are separated at appropriate delay time from the peak. Fig. 5 presents plots of measurements of the ΔQ/Q and electron equivalent energy (keV$_{ee}$). Through comparing the energy spectra, thermal neutron peak was confirmed at 366.85 ± 46.16 keV$_{ee}$. FOM for separating thermal neutron of ^{6}Li loaded scintillators at the thermal neutron energy region are shown in Table II.

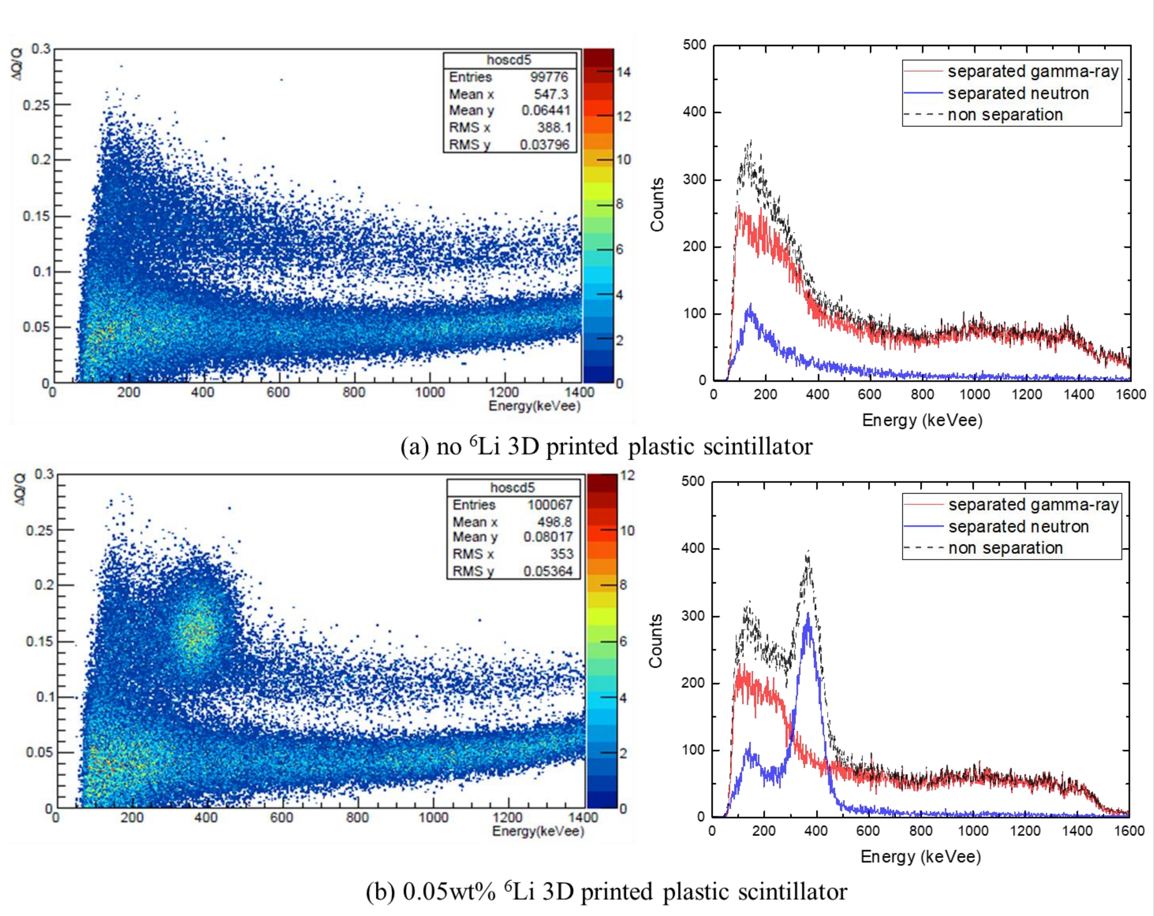

Fig. 5. PSD measurement of moderated ^{252}Cf source using 3D printed scintillators (left) and energy spectra separating n-γ through PSD (right).

Table II. Figure of merit of ^{6}Li loaded scintillators.

Scintillator	Thermal neutron energy region [keV$_{ee}$]	FOM
0.05wt% ^{6}Li	320-413	1.18 ± 0.029

Conclusion

3D printed scintillators were confirmed that could have PSD capability about thermal neutron and γ-ray through ^{6}LiF doping. The scintillators were evaluated with LO and FOM. The scintillator doped with 0.5wt%-^{6}Li was also attempted, but its performance was poor. The 0.5wt%-^{6}Li scintillator was lower LO and FOM than 0.05wt%-^{6}Li, as well as having poor resolution. The resolution was confirmed through thermal neutron energy region. It was considered to be attenuation by ^{6}LiF particles that were not completely decomposed. FOM of 0.05wt%-^{6}Li scintillator was 92.9% of useful FOM. It is expected that continuous research and optimization of compositions will make it possible to produce commercial-level thermal neutron detectable plastic scintillators by 3D-printing technique.

Reference

1. R.T. Kouzes, et al., "Neutron detection alternatives to ^{3}He for national security applications", Nuclear Instruments and Methods in Physics Research Section A: Accelerators, Spectrometers, Detectors and Associated Equipment, 623, 1035-1045 (2010).
2. N. Zaitseva, et al., "New solid-state organic scintillators for fast and thermal neutron detection", International Journal of Modern Physics: Conference Series, World Scientific, pp. 2060003, (2020).
3. Kyungmin Kim et al., "Neutron-Gamma Pulse Shape Discrimination Using 3D-Printed Plastic Scintillator with High-Concentration PPO", IEEE Nuclear Science Symposium and Medical Imaging Conference, Boston, October 31 – November 7, (2020).
4. Natalia Zaitseva, et al., "Pulse shape discrimination with lithium-containing organic scintillators", Nuclear Instruments and Methods in Physics Research, A 729, pp. 747-754 (2013).
5. N. Zaitseva, B.L. et al., "Plastic scintillators with efficient neutron/gamma pulse shape discrimination", Nuclear Instruments and Methods in Physics Research Section A: Accelerators, Spectrometers, Detectors and Associated Equipment, 668, 88-93 (2012).